

# Spin Spiral and Topological Hall Effect in a Metamagnet $\text{Fe}_3\text{Ga}_4$

Mahdi Afshar, and Igor I. Mazin

*Department of Physics and Astronomy, and Quantum Science and Engineering Center, George Mason University, Fairfax, VA 22030*

A new mechanism for Topological Hall Effect (THE) was recently proposed for the spiral magnet  $\text{YMn}_6\text{Sn}_6$ , which requires transverse conical spiral (TCS) magnetism, induced by external magnetic field, combined with thermally excite helical spiral magnons. In principle, this mechanism should be applicable to other itinerant spiral magnets as well. In this paper, we show that another metamagnetic compound,  $\text{Fe}_3\text{Ga}_4$ , where THE was observed experimentally before, in one of its phases satisfies this condition, and the proposed theory of thermal-fluctuation driven THE is quantitatively consistent with the experiment. This finding suggests that this mechanism is indeed rather universal, and the effect may have been observed in other compounds before, but overlooked.

## I. INTRODUCTION

During the last decades, topological effects driven by magnetic textures have attracted considerable attraction [1–5]. In particular, the Hall effect has been widely used as a probe for topological effects. In the classical Hall effect, discovered more than a century ago, the Lorentz force resulting from an external magnetic field gives rise to an electric field perpendicular to the electron current. The theory of this phenomenon is well known, and stipulates that the effect is linear in the magnetic field, with the ordinary Hall resistivity  $\rho^O = R_0 H$  (the proportionality coefficient  $R_0$  depends on the details of the Fermi surface). In systems with broken time-reversal symmetry (for instance, in ferromagnetic), there exists another contribution to the off-diagonal resistivity, dubbed “anomalous Hall effect” (AHE),  $\rho^A = R_s M$ . This contribution is proportional to the magnetization  $M$ , and gives rise to a Hall effect even in the absence of an externally applied magnetic field. While this relation is not always true, for instance, it is violated in some antiferromagnets [6], it has been routinely used to identify the AHE in the experiment.

Very recently an additional mechanism generating an off-diagonal resistivity in magnets with noncoplanar moments was identified [7]. Interestingly, contrary to the AHE, this mechanism does not require spin-orbit interaction, albeit can benefit from it [8]. This mechanism, often called Topological Hall Effect (THE) is based on the Berry phase an electron acquires when its spin follows a spatially varying magnetization that is present in such materials. It was shown that its amplitude is proportional to the so-called scalar spin chirality (SSC), defined as the triple product of three spins forming a triangle:

$$\Omega = \mathbf{S}_1 \cdot (\mathbf{S}_2 \times \mathbf{S}_3) \quad (1)$$

In principle, this mechanism is not supposed to work in system with zero SSC, and weak spin-orbit (as in many 3d metals). Yet, in several cases sizeable deviations from the standard formula,  $\rho = \rho^O + \rho^A = R_0 H + R_s M$ , were reported [9–12], and ascribed to THE, even though for all

these system the magnetic structure is known and does not have any SSC.

For one of this compound, namely  $\text{YMn}_6\text{Sn}_6$ , particularly detailed set of experimental data was available [10], and another mechanism for THE was proposed. Within this scenario, SSC emerges through a fluctuational mechanism akin to the emerging nematicity in Fe-based superconductor [13]. The resulting THE amplitude grows roughly linearly with temperature, with a quadratic dependence on magnetization. The prerequisites to this fluctuational THE (fTHE) are (a) a transverse conical spiral magnetic state at least in some range of temperatures and external fields (b) itinerant electrons strongly coupled with this spiral (ideally, formed by the same electron orbitals) and (c) strong fluctuations.

In this paper, we will study another compound where THE has been reported [9],  $\text{Fe}_3\text{Ga}_4$ , and will show that this observation is consistent with the same fTHE mechanism. In the following section we will describe the compound and the experimental picture, then we will present the results of our Density Functional Theory (DFT) calculations and discuss the magnetic phase diagram. After that, we will review the theory of the fTHE and apply it to  $\text{Fe}_3\text{Ga}_4$ .

## II. EXPERIMENTAL SITUATION

$\text{Fe}_3\text{Ga}_4$  crystallizes in a base-centered monoclinic structure, with the symmetry group  $C2/m$ , and a rather complex primitive unit cell of three formula units. The four crystallographically inequivalent Fe sites form seven parallel sheets along the  $c$ -direction as shown in Fig. 1, with interlayer distances of 0.368, 1.334, 1.104, 1.104, 1.334, 0.368 and 0.977 Å. The lattice parameters are  $a = 10.0979$  Å,  $b = 7.6670$  Å, and  $c = 7.8733$  Å with an obtuse angle of  $\beta = 106.298^\circ$  [9]. While crystallographically and electronically, as will be discussed in more details later, it is rather 3D, magnetically it can be viewed as a stack of ferromagnetically ordered planes with complex, but, presumably, weaker interplanar coupling [14].

The material is known to have two metamagnetic tran-

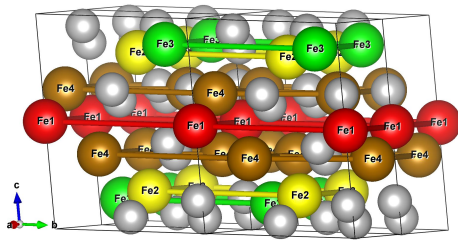


FIG. 1: (Color online) Layered structure of Fe atoms in  $\text{Fe}_3\text{Ga}_4$  crystal structure. The four different crystallographically inequivalent iron sites are shown in different colors. There are also four unique Ga sites, which are all shown in grey.

sitions [9, 14], from a ferromagnetic (FM) to a spin density wave (SDW) at  $T_1 = 60$  K, and back to a ferromagnetic state at  $T_2 \approx 360$  K (in this paper we apply the term SDW to any phase where spin polarization varies periodically in space; thus defined SDW can be either a spiral, or an *amplitude* SDW, wherein the magnitude of the magnetic moment varies continuously, or a combination of both). The long-range order is lost at  $T_3 = 420$  K. The nature of the SDW phase will be discussed later, we will just mentioned that the neutron data can be fit equally well [14, 15] by an *amplitude* SDW, where the spins are mostly aligned along  $c$ , or by a spin spiral, with the helical orientation, *i.e.*, with the spins rotating in the  $ab$  plane. Either way, the spiral wave vector appears to be  $(0, 0, 0.29)$ . The low- $T$  and the high- $T$  phases that are identified as ferromagnetic should be more correctly characterized as uncompensated magnetic phases. Especially the high- $T$  phase may be a noncollinear canted phase with zero net magnetization. In this paper, however, we will not be concerned with the natures of those phases, but only with the SDW phase between  $T_1$  and  $T_2$ .

Experimentally, the low-temperature ferromagnetic phase shows the lowest susceptibility in the fields below 0.3 T for the field direction along  $a$ , and the highest along  $c$ , but the  $c$  and  $b$  directions are nearly the same. This was interpreted [14, 15] as if  $a$  is the easy axis, and  $b$  is the hard one. On the first glance, this implies that the ground state in the SDW phase can be either amplitude wave with polarization along  $a$ , or a cycloidal spiral with the spins rotating in the  $ac$  plane. However, the latter is not compatible with the neutron data, therefore the authors of Ref. [14, 15] argued it must be an amplitude wave (note that in text of Ref. [14] it was incorrectly stated that the suggested SDW is linearly polarized along  $c$ , but the figure correctly shows the one polarized along  $a$  [15]). However, the difference between the  $c$ - and  $b$ -axis susceptibilities being at least five times smaller than that between  $c$  and  $a$ , an  $ab$  spin helix could not be reliably excluded.

While not explicitly discussed in Ref. [9], magnetometry clearly shows a spin-flop transition for the field  $H \perp c$ , which is not very distinctly defined (probably because of the sample quality), but is seen to occur in the SDW phase at the field  $H_b \gtrsim 1$  T at  $T = 150$  K, with  $H_b$  linearly decreasing with temperature down to  $\sim 0.5$  T at  $T \sim 300$  K. Careful examination of the  $M(H)$  curves for  $H \perp c$  suggests a possibility of another spin-flop transition, at very low fields  $H_a \lesssim 0.1$  T, but that is rather speculative.

The residual resistivity was relatively large, with the room-temperature ratio  $\sim 2$ , indicating a large number of defects and possibly deviations from stoichiometry. The residual specific heat coefficient  $C(T)/T|_{T \rightarrow 0} = 23$  mJ/mole K<sup>2</sup>, corresponding to the density of states (DOS) at the Fermi level  $N(0) \approx 10$  states/f.u.. Only the first phase transition, at  $T = T_1$ , has a distinct specific heat signature, and the entropy change is very small, less than 0.3% of  $R \log 2$ , indicating that the transition occurs between two well ordered states. The authors of Ref. [9] estimate that entropy change between  $T_2$  and  $T_3$  as 0.43 J/mole K, which is less than 10% of  $R \log 2$ , consistent with a quasi-2D character of magnetism in this material.

Transport measurements indicate an extra contribution for the Hall effect  $\rho_{xy}$  (*i.e.*, in a magnetic field in the  $ab$  plane) for an intermediate temperature range, roughly coinciding with the  $(T_1, T_2)$  interval, compared with the standard combination of an anomalous and an ordinary Hall effect,

$$\rho_{xy}(H) = R_o H + R_s M. \quad (2)$$

The coefficients  $R_o$  and  $R_s$  strongly depend on the phase, and, inside each phase, also depend on temperature, which makes it difficult to quantify the additional, presumably topological, contribution, but one can say with confidence that this contribution increases with temperature up to the highest reported temperature of 350 K.

### III. DFT CALCULATIONS

Calculations of the structural, electronic, and magnetic properties of bulk  $\text{Fe}_3\text{Ga}_4$  were performed using the Vienna *ab initio* simulation package (VASP) [16–19]. Fe 3s, 3p, 3d, and 4s and Ga 3p, 3d, and 4s states were treated as valence. The plane cut-off was 500 eV. We use the Gaussian smearing with the width of 0.05 eV, this value ensuring an entropy contribution to the free energy of less than 1 meV/atom. The generalized gradient approximation (GGA) was used for the exchange-correlation functional [21]. The spin-orbit coupling (SOC) was included in the self-consistent calculations, unless mentioned otherwise. The k-point sampling was based on a  $\Gamma$ -centered grid for all calculations and we used an optimized  $(10 \times 10 \times 10)$  k-points, except when for the density of states (DOS) calculations, where the  $12 \times 12 \times 9$  grid was utilized.

In addition, we used an all-electron Full-Potential Local Orbitals (FPLO) [20] package, which solves the fully relativistic Dirac equations [22]. The basis set included Fe(1s, 2s, 2p, 3s, 3p, 3d), and Ga(3s, 3p, 3d, 4s, 4p, 4d, 5s) states. The total energy converged to 0.001 meV. In order to address the possible effect of the on-site electron correlations, we employed the GGA+U method in the fully-localized limit [23]. As implemented in FPLO, it has full nonspherical double counting subtraction (as opposed to most other codes), whereby the first Slater integral is defined as  $F_0 = U$ , where  $U$  is the Hubbard repulsion, and the Hund's rule coupling defined the other integrals via  $J = (F_2 + F_4)/14$ , and the ratio of  $F_4/F_2$  is set to 0.625, typical for 3d transition metals [24]. We used  $J = 0.9$  eV, and varied  $U$ .

Spin spiral and unrestricted noncollinear calculations were performed using the VASP package. For the former, the generalized Bloch theorem formalism [25] was utilized, and verified against  $1 \times 1 \times 4$  unrestricted noncollinear calculations. By construction, the spiral formalism does not include the spin-orbit coupling, but relevant energy differences were similar to those in relativistic supercell calculations.

Fig. 2 summarizes the result of these calculations. We have scanned the irreducible part of the primitive Brillouin zone using the  $5 \times 5 \times 4$  mesh with the step of  $0.1 G$  from 0 to  $0.5G$  for each crystallographic direction ( $G$ 's are the corresponding reciprocal lattice vectors), altogether 216 calculations. One can see that the magnon spectrum is stiff along  $x$  and  $y$ , and soft along  $z$ , with a minimum close to  $\mathbf{q} = (0, 0, 0.27)$  in reciprocal lattice units. We then calculated the spiral energies with a finer mesh of  $7 \times 7 \times 7$ , along the line  $\mathbf{q} = (0, 0, q_z)$ , with a step of 0.02 in  $q_z$  (Fig. 2). The position of the minimum has not change. The value of  $\mathbf{q} = (0, 0, 0.27)$  agrees well with the experimental number.

We have also tried to stabilize an amplitudinal SDW, as suggested in Ref. [14]. It never stabilizes, indicating that the DFT ground state is resoundingly spiral.

While the FM Fermi surface does not show any visible nesting feature, nor does the non-interacting susceptibility (either  $\chi_{zz}$  or  $\chi_{+-}$ ) show any well-defined maximum, the calculated density of states for the FM ( $\mathbf{q} = 0$ ) and the spiral  $\mathbf{q} = (0, 0, 0.27)$  states (Fig. 3) show small spectral weight transfer from the region within a few tenths of an eV near the Fermi level to farther energies, that is, a small, but noticeable pseudogap effect.

We have also calculated the magnetic anisotropy as a function of the Hubbard correction  $U$  (calculations reported above were not including  $U$ ). To this end, we used the FPLO method, which treats the relativistic effects more accurately and the angular dependence of the GGA+U term is included in a more systematic way. The results are presented in Fig. 4. The calculated anisotropy for the Hubbard parameter of  $U$  from 1eV to 3eV and Hund's  $J = 0.9$  eV agrees with the experiment.

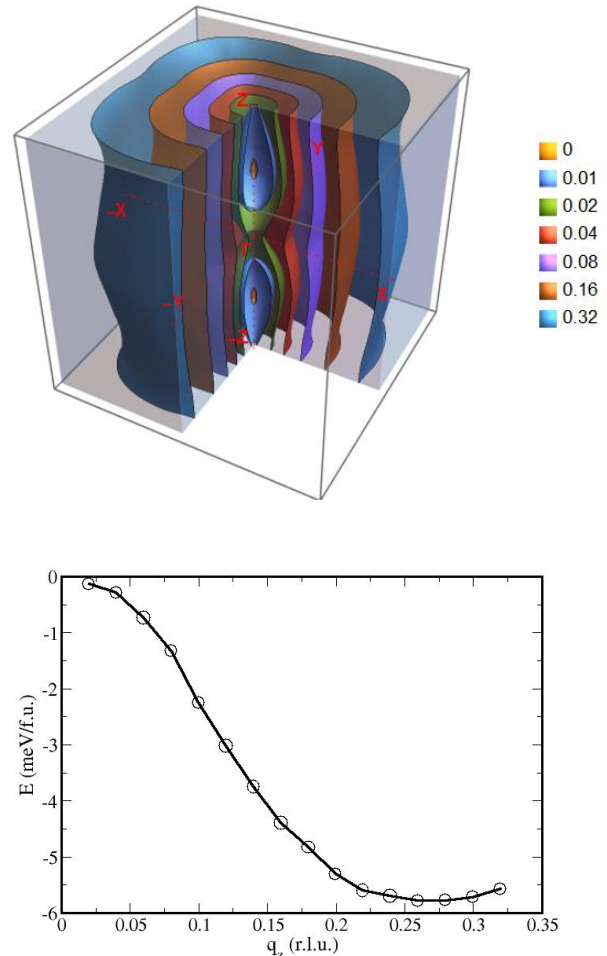


FIG. 2: (Top panel) 3D contour plot of the total energy of a non-relativistic spiral with a spiral vector  $\mathbf{q} = (x, y, z)$ , where  $x, y, z$  are components in reciprocal lattice coordinates. (Bottom panel) same, for the vector  $\mathbf{q} = (0, 0, z)$ .

Also, particularly at  $U \approx J$ , the difference between the  $c$  and  $b$  orientations is on the order of 0.1 meV/Fe, resulting in a stabilization energy for the cycloidal  $ac$  spiral about 0.05 meV.

One reason why the helical spiral may be more stable in the experiment is the dipole-dipole interaction [26]. Indeed, in the long-wave-length limit it contributes, for a cycloidal (but not helical) spiral an additional energy equal to  $\int \pi m^2 dV$ , where  $m$  is the magnetization density, and the integration is over the entire crystal. Using the  $\text{Fe}_3\text{Ga}_4$  parameters, we get an estimate of 0.06 meV/Fe, comparable with, and slightly larger than the electronic anisotropy energy.

In principle, the next step would be to attempt deriving a first principles Heisenberg Hamiltonian. In  $\text{Fe}_3\text{Ga}_4$ , unfortunately, it is virtually impossible because of too many inequivalent bonds and the fact that many ferrimagnetic

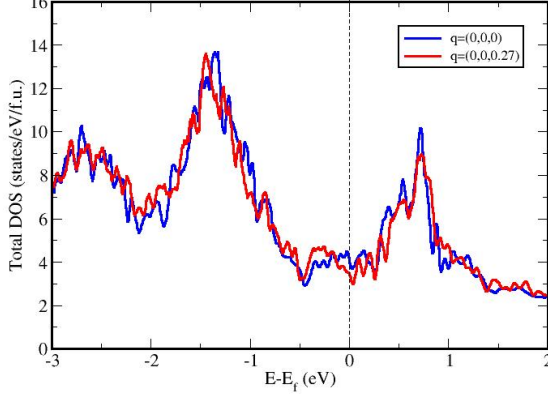


FIG. 3: Density of states near the Fermi level for the ferromagnetic  $[\mathbf{q} = (0, 0, 0)]$  and spiral  $[\mathbf{q} = (0, 0, 0.27)]$  states. Note small, but discernible weight transfer away from the Fermi level.

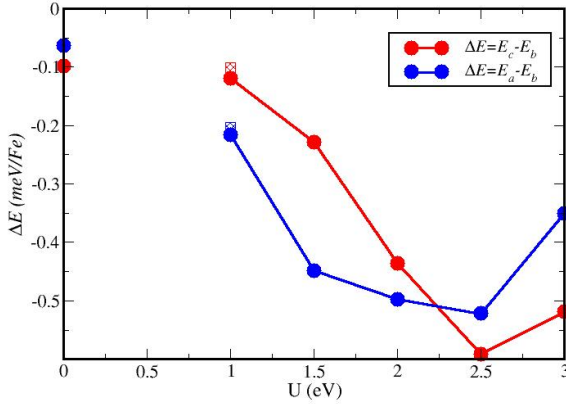


FIG. 4: Magneto-anisotropy energy for the quantization axis along the crystallographic  $a$ ,  $b$  and  $c$  axes. Calculations were performed in FPLO for the Hund's of  $J = 0.9$  eV as a function of Hubbard  $U$ . Zero corresponds to DFT calculations without the GGA+ $U$  correction. The two points for  $U = 1$  eV correspond to the  $k$ -point meshes of  $8 \times 8 \times 8$  and  $12 \times 12 \times 12$ .

configurations simply fail to converge. On the other hand, it appears that the SDW in  $\text{Fe}_3\text{Ga}_4$  can be quite well described in a continuous model. Indeed, as discussed above, a unit cell includes 9 Fe atoms arranged in 7 separate  $ab$  Fe layers stacked along  $c$ . Our spin-spiral calculations place no restriction on the mutual orientation of their magnetic moments. Yet, the self consistent solution can be very accurately described by a simple sinusoid, where the helix angle is given by  $\alpha(z) = \cos(0.27 \times 2\pi z/c)$  (Fig.

5). Only the two Fe3 layers slightly deviate from this formula.

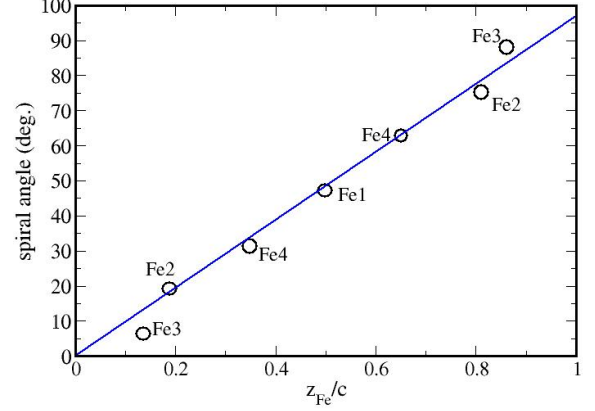


FIG. 5: Spiral angle as function of the position of an Fe layer within the unit cell, for the spiral calculations with  $\mathbf{q} = (0, 0, 0.27)$ . No restrictions are imposed on the magnetic moment directions within a single unit cell, while the consecutive unit cells are rotated by  $0.27 \times 360^\circ$ . The line shows the ideal sinusoid,  $\alpha = 0.27 \times 360^\circ z$ .

Interestingly, the calculated energy as a function of the spiral vector is very well described by the function

$$E = E_0 + J_1 \cos 2\pi qh + J_2 \cos 4\pi qh, \quad (3)$$

where  $h = 1.75$ ,  $J_1 = 3$  meV and  $J_2 = 0.4$  meV, as if the Hamiltonian was comprised of two antiferromagnetic Heisenberg interaction, one acting across the distance of  $1.75c$  and the other of  $3.5c$ . Of course, in reality this would be only an effective Hamiltonian, resulting from concerted action of all sorts of exchange interactions, but it indicates that the overall magnetic coupling is extremely long range.

In any event, the calculations unambiguously indicate that of the two possible ground states compatible with the neutron scattering data it is the helical spiral that is realized, and not an amplitude SDW.

#### IV. TOPOLOGICAL HALL EFFECT

Typically, the Hall effect in metals is described as a sum of two components: the ordinary Hall effect [27], stemming from the Lorentz force experienced by the charge carriers, and the anomalous Hall effect [27], resulting from the interplay between the exchange field and spin-orbit coupling. While there are notable exceptions (in particular, the anomalous Hall effect was shown to exist even in some systems with zero magnetization [6]), it is customary to assume that the ordinary Hall resistance is proportional

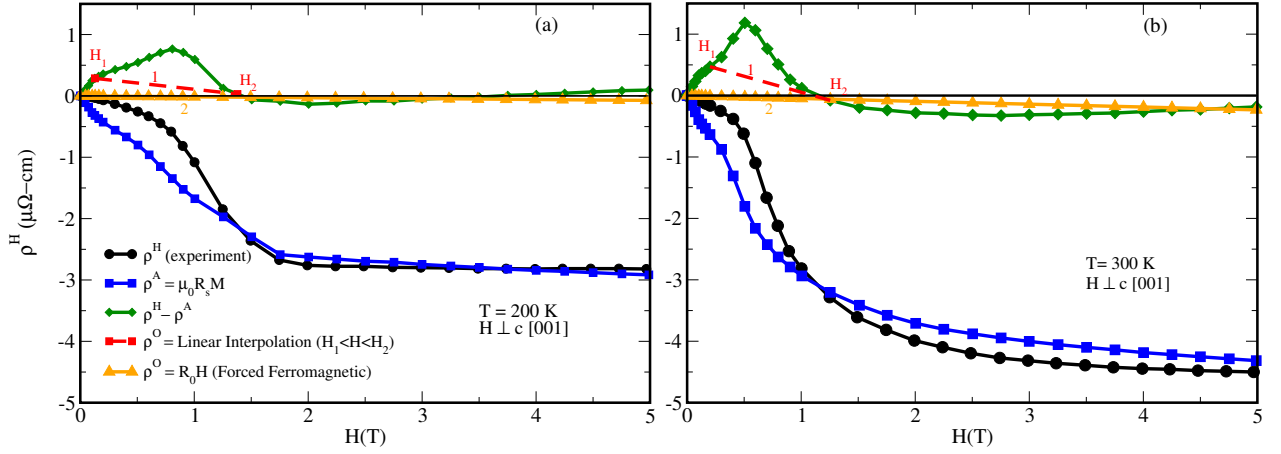


FIG. 6: Suggested decomposition of the Hall resistivity measured by Mendez *et al.* [9], for two different temperatures.

to the applied field,  $\rho^O = R_0 H$ , and the anomalous to the net magnetization,  $\rho^A = R_s M$ . Recently it was pointed out that in noncoplanar magnets a third term should be added (see, for instance, Ref. [7], called topological Hall effect (THE), proportional to the so-called scalar spin chirality  $s$ , which can be defined in a discrete representation as a triangular loop over near-neighbor magnetic moment,  $s = \mathbf{M}_1 \cdot (\mathbf{M}_2 \times \mathbf{M}_3)$ .

In the continuous representation one can define the topological field,

$$b_i(\mathbf{r}) = \sum_{jk} e_{ijk} \mathbf{M}(\mathbf{r}) \cdot \left( \frac{\partial \mathbf{M}(\mathbf{r})}{\partial r_i} \times \frac{\partial \mathbf{M}(\mathbf{r})}{\partial r_k} \right) \quad (4)$$

$$= \sum_{jk} \sum_{\alpha\beta\gamma} e_{ijk} e_{\alpha\beta\gamma} M_\alpha \frac{\partial M_\beta}{\partial r_i} \frac{\partial M_\gamma}{\partial r_k} \quad (5)$$

where  $i, j, k$  are Cartesian indices in the real space, and  $\alpha, \beta, \gamma$  in the spin space. This field can couple with the external magnetic field and generate an additional contribution to the Hall resistivity in the field parallel to  $\mathbf{b}$  [7]. As a result, the Hall resistivity is commonly written as:

$$\rho^H = R_0 H + R_s M + \rho^T, \quad (6)$$

It is well known that a nonzero topological field  $\mathbf{b}$  can be generated by a linear combination of three (but not two) helical spirals [28]. It was recently pointed out[10] that a combination of two spirals, one of which is helical, and the other transverse conical, can have a nonzero topological field. Further more, Ghimire *et al*[10] argued that even if the ground state is a *single* helical spiral propagating along a given direction, say,  $z$ , in a suitable magnetic field  $\mathbf{H} || \mathbf{x} \perp \mathbf{z}$  this spiral is liable to flop into a transverse conical spiral, propagating along  $z$  and canted toward  $x$ . Furthermore, it was also shown [10] that spin fluctuations in form of a helical magnon propagating along  $y$  can be selectively excited, generating a topological field

(and hence the topological Hall effect) proportional to the temperature and also dependent on the net magnetization. In Ref. [10] a simple formula was derived, which reads

$$\rho^T = \kappa(1 - M^2/M_s^2)TH, \quad (7)$$

where  $\kappa$  is an unknown, material-specific constant, and  $M_s$  is the saturation magnetization.

However, direct substitution of Eq. 7 into Eq. 6 is not possible, for the reason that the assumption that  $R_0$  and  $R_s$  do not depend on magnetic field is, while popular, generally incorrect. Both coefficients are determined by the electronic structure, which, in turn, is very sensitive to magnetic order. This problem was discussed in Ref. [10] where the following protocol was worked out: First, the Hall resistivity in the non-topological phases below (in terms of the external field  $H$ ) or above the topological phase ( $H_1 < H < H_2$ ) are fit separately to the first two terms in Eq. 6. In principle, they should be then continuously connected to each other across the topological region and the subtracted from the total  $\rho^H$ . In Ref. [10], for the lack of any justifiable recipe, they were simply connected by the straight line. Now, since the difference, which we will call  $\rho^T$ , is, by construction, zero at  $H_1$  and  $H_2$ , they subtracted the linear base  $\rho_0 = [(H - H_1)\rho^T(H_2) + (H_2 - H)\rho^T(H_1)]/(H_2 - H_1)$ , where  $\rho^T(H)$  was taken from Eq. 7.

We have followed this protocol, albeit the experimental data are not nearly as clean as in  $\text{YMn}_6\text{Sn}_6$  ( $\text{Fe}_3\text{Ga}_4$  is known to form with considerable disorder), in particular, proper identification of the first and the second spin-flop fields is difficult. Still, we were able to tentatively assign them to be (see Fig. 6), at  $T = 200$  K,  $H_1 \approx 0.125$  T and  $H_2 \approx 1.375$  T, and at  $T = 300$  K,  $H_1 \approx 0.18$  T,  $H_2 \approx 1.25$  T (at lower temperatures the topological signal is too weak to be analyzed quantitatively). The results of this analysis are shown in Fig. 7. Note that the amplitude of the topological signal is about 40% higher at  $T = 300$  K, in good agreement with  $300/200 = 1.5$ ,



consistent with the linear dependence on  $T$  in Eq. 7.

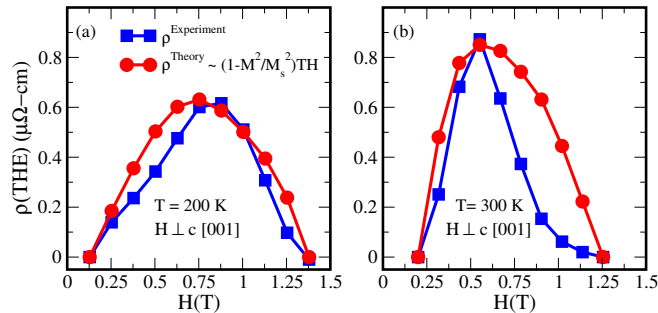


FIG. 7: Topological Hall effect resistivity extracted as described in the text, compared to Eq. 7

## V. CONCLUSIONS

We have studied, using Density Functional Theory, magnetic properties of a potential topological-Hall material,  $\text{Fe}_3\text{Ga}_4$  metal. We found that the DFT ground state is a spin spiral, propagating along the crystallographic  $c$  direction with  $\mathbf{q} = (0, 0, 0.27)$  reciprocal lattice units. This is in excellent agreement with the neutron scattering findings for temperatures above  $\sim 100$  K. Contrary to the previously published conjecture we identified this state as a spiral, and not an amplitude spin density wave. We argue that the actual ground state, despite  $b$  being (slightly) the hard magnetic axis, is an  $ab$  helical spiral, stabilized by dipole-dipole interactions.

We have further identified a spin flop field at which the helical spiral flops into a transverse conical spiral, which, according to the theory proposed recently by one of us for another topological-Hall spiral magnet,  $\text{YMn}_6\text{Sn}_6$ . The same theory works well for  $\text{Fe}_3\text{Ga}_4$ . Indeed, the theory predicts a topological Hall effect in the transverse conical phase only, with a strong (approximately linear) temperature dependence, and both predictions are corroborated by the experiment. This, second observation of the dynamically fluctuation-induced topological Hall effect, strongly suggests that the proposed theory is correct and sufficiently universal.

## ACKNOWLEDGMENTS

The authors acknowledge funding from the U.S. Department of Energy through Grant No. DE-SC0021089. We also acknowledge the Department of Defense (DoD) Major Shared Computing Resource Center at Air Force Research Laboratory (AFRL) and the National Energy Research Scientific Computing Center (NERSC) for high-performance computing facilities, where some portions of the calculations were performed. Last but not least, we

acknowledge many insightful discussions with Huibo Cao and Maxim Mostovoy.

- [1] J. Zang, V. Cros, and A. Hofmann, eds., *Topology in Magnetism*, Springer, Cham, (2018).
- [2] N. Nagaosa, and Y. Tokura, *Topological properties and dynamics of magnetic skyrmions*, Nature Nanotechnology **8**, 899 (2013).
- [3] N. Nagaosa, X.Z. Yu, and Y. Tokura, *Gauge fields in real and momentum spaces in magnets: monopoles and skyrmions*, Phil. Trans. R. Soc. A, **370**, 5806 (2012).
- [4] B. Bradlyn, J. Cano, Z. Wang, M. G. Vergniory, C. Felser, R. J. Cava, and B. A. Bernevig, *Beyond Dirac and Weyl fermions: Unconventional quasiparticles in conventional crystals*, Science, **353**, aaf5037 (2016).
- [5] N.P. Armitage, E.J. Mele, and A. Vishwanath, *Weyl and Dirac semimetals in three-dimensional solids*, Reviews of Modern Physics **90**, 15001 (2018).
- [6] L. Šmejkal, R. González-Hernández, T. Jungwirth, J. Sinova, *Crystal time-reversal symmetry breaking and spontaneous Hall effect in collinear antiferromagnets*, Science Advances **6**, eaaz8809 (2020).
- [7] P. Bruno, V.K. Dugaev, and M. Tailleferrier, *Topological Hall Effect and Berry Phase in Magnetic Nanostructures*, Phys. Rev. Lett. **93**, 096806 (2004); N. Nagaosa, Y. Tokura, *Topological properties and dynamics of magnetic skyrmions*, Nature Nanotechnology, **8**, 899, (2013).
- [8] S.S. Zhang, H. Ishizuka, H. Zhang, G.B. Halász, and C.D. Batista, *Real-space Berry curvature of itinerant electron systems with spin-orbit interaction*, Phys. Rev. B **101**, 024420 (2020).
- [9] J.H. Mendez, C.E. Ekuma, Y. Wu, B.W. Fulfer, J.C. Prestigiacomo, W. A. Shelton, M. Jarrell, J. Moreno, D. P. Young, P. W. Adams, A. Karki, R. Jin, Julia Y. Chan, and J. F. DiTusa, *Competing magnetic states, disorder, and the magnetic character of  $\text{Fe}_3\text{Ga}_4$* , Phys. Rev. B **91**, 144409 (2015).
- [10] N.J. Ghimire, R.L. Dally, L. Poudel, D.C. Jones, D. Michel, N. Thapa Magar, M. Bleuel, M.A. McGuire, J.S. Jiang, J.F. Mitchell, J.W. Lynn and I.I. Mazin, *Competing magnetic phases and fluctuation-driven scalar spin chirality in the kagome metal  $\text{YMn}_6\text{Sn}_6$* , Sci. Adv., **6**, eabe2680, (2020).
- [11] G. Gong, L. Xu, Y. Bai, Y. Wang, S. Yuan, Y. Liu, and Z. Tian, *Large topological Hall effect near room temperature in noncollinear ferromagnet  $\text{LaMn}_2\text{Ge}_2$  single crystal*, Phys. Rev. Materials **5**, 034405, (2021).
- [12] Q. Wang, K.J. Neubauer, Ch. Duan, Q. Yin, S. Fujitsu, H. Hosono, F. Ye, R. Zhang, S. Chi, K. Krycka, H. Lei, and P. Dai, *Field-induced topological Hall effect and double-fan spin structure with a  $c$ -axis component in the metallic kagome antiferromagnetic compound  $\text{YMn}_6\text{Sn}_6$* , Phys. Rev. B **103**, 014416, (2021).
- [13] I.I. Mazin and J. Schmalian, *Pairing Symmetry and Pairing State in Ferropnictides: Theoretical Overview*, Physica C., **469**, 614 (2009).
- [14] Y. Wu, Z. Ning, H. Cao, G. Cao, K.A. Benavides, S. Karna, G.T. McCandless, R. Jin, J.Y. Chan, W.A. Shelton, J.F. DiTusa, *Spin density wave instability in a ferromagnet*, Sci. Rep., **8**, 5225 (2018).

- [15] H. Cao, private communication
- [16] G. Kresse and J. Hafner, *Ab initio molecular dynamics for liquid metals*, Phys. Rev. B **47**, 558 (1993).
- [17] G. Kresse and J. Hafner, *Ab initio molecular-dynamics simulation of the liquid-metal-amorphous-semiconductor transition in germanium*, Phys. Rev. B **49**, 14251 (1994).
- [18] G. Kresse and J. Furthmüller, *Efficient iterative schemes for ab initio total-energy calculations using a plane-wave basis set*, Phys. Rev. B **54**, 11169 (1996).
- [19] G. Kresse and J. Furthmüller, *Efficiency of ab-initio total energy calculations for metals and semiconductors using a plane-wave basis set*, Comput. Mater. Sci. **6**, 15 (1996).
- [20] K. Koepernik, H. Eschrig, FPLO-18: improved version of the original FPLO code, *Full-potential nonorthogonal local-orbital minimum-basis band-structure scheme*, Phys. Rev. B **59**, 1743 (1999), <http://www.fplo.de>.
- [21] J. P. Perdew, K. Burke, and M. Ernzerhof, *Generalized gradient approximation made simple*, Phys. Rev. Lett. **77**, 3865 (1996).
- [22] I. Opahle, Ph.D. thesis, TU Dresden, 2001; H. Eschrig, M. Richter, and I. Opahle, *Relativistic electronic structure theory. part II: Applications*, edited by P. Schwerdtfeger, Elsevier, Amsterdam, pp:723-776, (2004).
- [23] E.R. Ylvisaker, W.E. Pickett, K. Koepernik, *Anisotropy and magnetism in the LSDA+U method*, Phys. Rev. B **79**, 035103 (2009).
- [24] V.I. Anisimov, I.V. Solovyev, M.A. Korotin, M.T. Czyzyk and G.A. Sawatzky, *Density-functional theory and NiO photoemission spectra*, Phys. Rev. B **48**, 16929 (1993).
- [25] L.M. Sandratskii, *Energy band structure calculations for crystals with spiral magnetic structure*, Phys. Status Solidi B **136**, 167 (1986).
- [26] We thank Maxim Mostovoy for pointing out to us this possibility.
- [27] C.M. Hurd, *The Hall Effect in Metals and Alloys*, The International Cryogenics Monograph Series, Springer, (1972).
- [28] S. Mühlbauer, B. Binz, F. Jonietz, C. Pfleiderer, A. Rosch, A. Neubauer, R. Georgii, and P. Böni, *Skyrmion Lattice in a Chiral Magnet*, Science **323**, 915 (2009).